A multiplexed, single-cell sequencing screen identifies compounds that increase neurogenic reprogramming of murine Muller glia.

Amy Tresenrider[1], Marcus Hooper[2], Levi Todd[2], Faith Kierney[2], Nicolai Blasdel[2], Cole Trapnell[*,1,3,4], Thomas A. Reh[*,#,2]

[1]Department of Genome Sciences, University of Washington, Seattle, WA 98195, USA

[2]Department of Biological Structure, University of Washington, Seattle, WA 98195, USA

[3]Brotman-Baty Institute for Precision Medicine, University of Washington, Seattle, WA 98195, USA

[4]Allen Discovery Center for Cell Lineage Tracing, Seattle, WA 98195, USA

*Thomas A. Reh and Cole Trapnell

Email: tomreh@uw.edu, coletrap@uw.edu

Author Contributions: Conceptualization, AT, MH, LT, TR, Methodology, AT, MH, LT, Formal Analysis, AT, MH, LT, Investigation, AT, MH, LT, FK, NB, Writing-Original Draft, AT, LT, TR, Writing-Review & Editing, AT, MH, LT, CT, TR, Visualization, AT, LT, Supervision, CT, TR, Funding Acquisition CT, TR

Competing Interest Statement: C.T. is a SAB member, consultant and/or co-founder of Algen Biotechnologies, Altius Therapeutics, and Scale Biosciences. One or more embodiments of one or more patents and patent applications filed by the University of Washington may encompass methods, reagents, and the data disclosed in this manuscript. Some work in this study is related to technology described in patent applications.

Classification: Biological Sciences, Neurosciences

Keywords: single-cell sequencing, retina, reprogramming, cell signaling, neuron

This PDF file includes:

> Main Text
> Figures 1 to 3

Abstract

Retinal degeneration in mammals causes permanent loss of vision, due to an inability to regenerate naturally. Some non-mammalian vertebrates show robust regeneration, via Muller glia (MG). We have recently made significant progress in stimulating adult mouse MG to regenerate functional neurons by transgenic expression of the proneural transcription factor Ascl1. While these results showed that MG can serve as an endogenous source of neuronal replacement, the efficacy of this process is limited. With the goal of improving this in mammals, we designed a small molecule screen using sci-Plex, a method to multiplex up to thousands of single nucleus RNA-seq conditions into a single experiment. We used this technology to screen a library of 92 compounds, identified, and validated two that promote neurogenesis *in vivo.* Our results demonstrate that high-throughput single-cell molecular profiling can substantially improve the discovery process for molecules and pathways that can stimulate neural regeneration and further demonstrate the potential for this approach to restore vision in patients with retinal disease.

Main Text

Introduction

In mammalian species, retinal neurodegeneration results in permanent visual impairment because the central nervous system (CNS) lacks an endogenous regenerative capacity. By contrast, many non-mammalian vertebrates can replace lost neurons via neurogenic reprogramming of non-neuronal cells (1). Efforts to stimulate neural cell replacement in mammals, akin to what occurs in regenerative species, have been met with some success (2, 3). These approaches are typically focused on using transcription factors to reprogram glial cells into neurogenic precursors in contexts across the CNS (brain, retina, spinal cord). However, the reprogramming is incomplete, affecting only a subset of cells or producing cells without mature neuronal markers. Given the vast array of small molecules and biologics available, there is potential to screen for factors that improve such gene therapy techniques. Scalable methods capable of screening an increased number of reprogramming treatments have the potential to uncover factors that improve the regenerative potential of the mammalian CNS. These efforts may lead to future cell-replacement therapeutics.

We have recently developed methods to stimulate the regeneration of neurons from Muller glia (MG) in the mammalian retina *in vitro* and *in vivo* (2, 4–8). The *in vitro* viral overexpression of Ascl1 in primary MG is able to reprogram glia from young mice to acquire a neurogenic progenitor state and generate neurons (4, 9), and similar results have been obtained with brain astrocytes (4, 9). Ascl1 can also stimulate a neurogenic state in MG *in vivo* using a transgenic mouse line that targets this transcription factor (TF) specifically to MG. When these mice are subjected to retinal injury using a neurotoxic dose of NMDA and subsequently treated with histone-deacetylase inhibitors, the MG regenerate functional neurons in adult mice (2). Follow-up studies combining Ascl1 with other TFs have proven useful in stimulating glia to regenerate alternate arrays of neuronal fates (6, 7). These findings have established glia as a promising source for new neurons that could potentially be used to treat neurodegenerative disorders; however, the efficacy of neurogenesis is often too low to provide enough cells for functional recovery. Several studies have shown that cell signaling molecules can also affect the process of reprogramming cell fates, and investigators have suggested that small molecules might be useful in optimizing this approach for clinical applications of neural repair in combination or separate from TF overexpression (5, 9–12).

To identify additional compounds that aid in the reprogramming process and further stimulate neurogenesis from MG-derived progenitors, we set forth to design an assay that could scale the number of small molecules tested in a given *in vitro* experiment. Several limitations had made such plate-based screening difficult in the past: (1) screening was performed using marker genes and required the design of specific mice or cell lines to detect the emergence of only a single cell type; (2) MG are not a large population of cells in the retina of young mice, thus the

2

starting material is limited; and (3) current imaging-based methods to quantify the reprogramming outcome are low throughput. While traditional single-cell sequencing methods enable the molecular characterization of all cell types in a culture using low cell input without the need for marker genes, they are too costly for most labs to perform for more than a handful of samples. sci-Plex, a combinatorial indexing-based technology, scales the number of samples within a given single-cell sequencing experiment to up to thousands of samples, overcoming such limitations (13)(13, 14). However, current applications of sci-Plex have been performed in combination with the high throughput sci-RNA-seq3 protocol using culturing systems or organisms in which cell number is not limited (13, 15–17). Here we demonstrate that sci-Plex is also compatible with lower input samples in combination with the sci-RNA-seq2 protocol which requires a lower cell input and has a higher cell recovery rate.

Our application of sci-Plex to reprogramming MG is the first demonstration of sci-Plex's utility for screening chemical compounds in a low abundance primary cell type with disease relevance. To examine and validate the utility of sci-Plex for this purpose, we applied sci-Plex to MG exposed to Ascl1 overexpression for different timings and durations. We saw that, increasing the length of Ascl1 exposure increased the number of neurons produced, and we uncovered molecular features associated with progression towards the neuronal fate. When we applied sci-Plex to a small molecule screen for factors associated with stem cell biology, we uncovered compounds that had effects on neurogenesis and total cell recovery. Several of the most effective compounds identified *in vitro* were further tested *in vivo* in a reprogramming assay where Ascl1 is over-expressed specifically in MG (i.e. ANT protocol). The results of this secondary *in vivo* screen identified two compounds that significantly enhanced neurogenesis in adult mouse retina.

Results

sci-Plex captures the in vitro temporal dynamics of neurogenic reprogramming from MG

We first aimed to assess the ability of sci-Plex to assign cells to specific wells in an expected manner by observing the *in vitro* kinetics and dynamic gene expression program of Ascl1-dependent MG reprogramming. Retinas were isolated from P11 mice expressing a constitutive rtTA driving a tet-inducible Ascl1-GFP. The retinas were dissociated and grown as previously described to enrich for MG (4). We have previously shown that induction of Ascl1, by addition of doxycycline to the medium, induces neurogenesis in the MG, and that the new neurons generated from the reprogrammed MG most closely resemble bipolar neurons (4) (**Fig. 1A**). Taking advantage of the ease by which condition number can be scaled with sci-Plex, we induced Ascl1 in replicate for 1-5 days at varying windows of time, allowing us to temporally track the conversion of MG to neurons (**Fig. 1A-B**). Upon collection, nuclei were isolated in their individual treatment wells, the nuclei were barcoded with well-specific polyadenylated oligonucleotides "hashes", and then pooled for sci-RNA-seq2 (13, 14). We recovered 12,850 cells across two experiments and 30 wells (Timecourse: 7,004, Pulse: 5,846) with a median UMI count of 3,172 and 2,398 after all filtering steps, respectively (**Fig. S1 A-K**). The hash recovery rate was 68% for both experiments (**Fig. S1C-D, G-H**). The experiments were integrated and visualized by UMAP using Monocle3 (14, 18). The clusters were annotated according to cell type using the expression of known marker genes (**Fig. S1L-N, Table S1**) (14, 18). Most cells fell into one of four clusters: (1) MG; (2) Progenitor-like cells (ProL); (3) Transition; and (4) neuronal precursors (NeuPre). In addition, we identified other clusters of non-MG derived cells, including microglia, astrocytes, and fibroblast-like cells (FibroL), potentially derived from vascular cells (**Fig. 1C**).

Having annotated the cells, we next ordered all the cells originating from reprogrammed MG into a pseudotime trajectory to better understand the sequence of gene regulatory events on the path from MG to neuronal identity (**Fig. 1D**). We then assessed how the timing and duration of Ascl1 overexpression affected reprogramming progression when Ascl1 was added continuously (Timecourse) or pulsed (Pulse). In the Timecourse experiment, Ascl1 expression was induced for either 0,1,2,3,4 or 5 days and then the cells were collected (**Fig. 1B**). During the timecourse, we saw that Ascl1 stimulated a rapid transition away from MG (i.e. the start of the pseudotime

trajectory) that persisted across all timepoints (**Fig. 1E**). As expected, increased duration of Ascl1 overexpression led to cells further along the pseudotime trajectory, consistent with the need for Ascl1 expression to drive cells from the ProL state towards the neuronal state.

In the Pulse experiment, we initiated Ascl1 expression in all samples at the same time, but then removed doxycycline after either 1, 2, 3, 4, or 5 days to shutdown Ascl1 overexpression. The cells were all collected 5 days after the start of Ascl1 expression regardless of Ascl1 expression duration (**Fig. 1B, Pulse**). When Ascl1 was maintained for the entire 5 day period (**Fig. 1D-E**), the distribution of cells across pseudotime was similar to that observed in the Timecourse experiment, with few MG remaining. However, the pseudotime profiles were remarkably different when Ascl1 overexpression was removed for any period of time for all cell types with the exception of NeuPre (**Fig. S1Q**). When Ascl1 was expressed in the cells for 2 or fewer days, almost all of the cells were identified as MG (**Fig. 1E-F**). After 3 or more days of Ascl1 expression, transition and neurogenic precursor (NeuPre) cells began to accumulate, though a substantial number of MG were also present even after 4 days of Ascl1 exposure and one day without when compared to the Timecourse experiment (**Fig. 1F, Fig S1Q**). These results suggest that even after 4 days of Ascl1 expression, removal of Ascl1 allows a subset of the cells to return to a glial state, while another subset of cells that have made it far enough along the reprogramming trajectory are no longer dependent on Ascl1 to remain committed to their neuronal fate.

To further understand the molecular features of the cells as they progress towards a more neuronal fate, we analyzed changes in gene expression around the pseudotime stage associated with a decreased reliance on Ascl1. We found the local minima (10 < pseudotime < 20) of pseudotime density plots from the Pulse experiment to be 16 (**Fig S1R**). The accumulation of cells with a pseudotime value of > 16 encompasses the population of cells that remain in the NeuPre or Bipolar fate even after removal of Ascl1 induction. Coincidentally, in the Timecourse experiment, decreased Ascl1 expression is observed at pseudotime values > 16 (**Fig. S1S**). While seemingly surprising, this decrease in Ascl1 expression with continued exposure to the induction signal is a phenomenon we consistently observe in both our in vitro and in vivo reprogramming paradigms (Todd et al. 2021; Todd et al. 2022; Todd et al. 2020). We do not have definitive knowledge of the mechanism behind how Ascl1 expression is repressed, but it is possible that mature neurons have a mechanism to downregulate it.

To find the genes dynamically expressed during the loss of Ascl1 expression and gain of a more neuronal fate, we performed differential gene expression analysis across pseudotime using cells with pseudotime values from 10-20 (**Dataset S1**). We were particularly interested in identifying transcriptional regulators and signaling molecules. In the top 250 most differentially expressed genes, three major regulatory patterns (Cluster 1: increasing, Cluster 2: a transient increase, Cluster 3: decreasing) were observed (**Fig. 1G-H**). The downregulation of Id1 and Id3 in Cluster 2 was consistent with known biology: these factors (1) form heterodimers with bHLH TFs making them incapable of binding their target sites (19) and (2) have been previously implicated in maintaining retinal progenitors and Muller glia in a progenitor-state (2, 4–8). Genes in Cluster 1, which increase during the progenitor-to-neuron transition, are also associated with the normal development of neurons (Elavl3, Map2) and with processes such as neuronal maturation and synaptogenesis (Nrxn3, Syt1). There were also four TFs that increased in their expression right around the loss of Ascl1 dependence: Sox4, Neurog2, Myt1, and Rorb. All of these genes are expressed in the retina during the early stages of neurogenesis (20–25). Of note, Myt1 is a direct target of Ascl1 and although it has been studied more thoroughly in the brain, it is associated with repression of progenitor gene expression programs (20, 21). Another factor on the list, Rorb is involved in the specification of photoreceptor, amacrine, and horizontal but not bipolar cell fates (26, 27). Our results thus show the ability of sci-Plex to be used in MG cultures and we have identified potential regulators of critical steps in the MG to neuron reprogramming paradigm.

sci-Plex as a screen to identify small molecules that affect Ascl1-dependent MG reprogramming

The above results supported the potential of sci-Plex to study neurogenic reprogramming, so we next embarked on a larger-scale screen for factors that can improve the efficiency of neurogenesis

from MG. We screened through 92 small molecules from the TocriScreen Stem Cell Library (**Dataset S2**). The compounds target a range of biological functions with a bias towards epigenetic modulators and modulators of common signaling pathways (**Fig. 2A**). We followed the same treatment regime as for the timecourse experiment in which MG were isolated from P11 mice that express a constitutive rtTA and harbor a tet-inducibe Ascl1-GFP. The MG were selectively cultured before induction of Ascl1 with doxycycline. Small molecules from the TocrisScreen Stem Cell Library were added at the same time as the doxycycline and remained in culture until the cells were collected on Day 5 (**Fig. 2B**). The compounds were applied across three doses (0.1, 1, and 10 uM) with each compound being tested on one of two different collection days. We included three wells per collection day in which only doxycycline was added (Only Ascl1) and three wells per collection day in which doxycycline was not added (No Ascl1). To maximize the range of compounds tested, we opted to perform the sci-Plex experiment once, and then follow up with compounds that elicited strong effects through subsequent *in vivo* validation experiments. In sum, we screened 92 small molecules and two control conditions from a total of 265 individual wells after filtering out conditions with low cell recovery.

We used sci-RNA-seq2 to profile a total of 27,152 cells (Collection 1: 6,282, Collection 2: 20,870) (**Fig. S2A-G**). The median UMI count was 3,551 for Collection 1 and 2,166 for Collection 2 (**Fig. S2H-I**). A hash could be called for 65-74% of the cells (**Fig. S2F**). We performed dimensionality reduction and clustering with Monocle3 and used marker genes to annotate cell types by cluster. All cell types not of retinal/MG origin were discarded (**Fig. S2J-L**), and the dimensionality reduction and cell type annotation was repeated (**Fig. 2C, Table S1**).

To identify the molecules most likely to promote reprogramming, we pooled the clusters corresponding to neurogenic precursors (NeuPre: Gap43, Snap25, Dcx) and bipolar neurons (BP: Snap25, Vsx2, Cabp5, Otx2, Grik1) together into a common Neuron annotation and for each drug, calculated the abundance of Neurons relative to Ascl1(**Fig. 2D** and **Dataset S2**). Many of the molecules did not have clear effects on the reprogramming process. However, we found several molecules that increased neurogenesis and others that reduced neurogenesis. The molecules that most markedly increased the percentage of Neurons, included DBZ (28), DMH-1 (29), RepSox (30, 31), SB 431542 (32, 33), and WH-4-023 (34–36). These compounds target one of three molecular signaling pathways: Notch, BMP/TGF-beta, and LCK/SRC. We also calculated the number of cells recovered per well, and noticed that for a few treatments, far more total cells, regardless of cell type identity, were recovered than average. This was most prominent for metformin, sodium 4-phenylbutyrate, and valproic acid (**Fig. 2E**). Both sodium 4-phenylbutyrate and valproic acid are HDAC inhibitors which is of interest because TSA, another HDAC inhibitor, is a significant stimulus for Ascl1-dependent reprogramming *in vivo* (2). Unexpectedly, metformin, a compound that is approved for the treatment of diabetes with other potential clinical uses(37), also increased cell recovery in our assay. Because metformin has not been evaluated in the context of retinal reprogramming, we decided to pursue it and the 5 compounds that increased neurogenesis with further experiments *in vivo*. Thus, the use of sci-Plex aided us in narrowing down 92 compounds to 6 for follow up investigations.

In addition to detecting shifts along the reprogramming trajectory, we also detected what appeared to be previously undetected cell states (**Fig. 2C, Unknown clusters**). To characterize these, we performed Biological Process GO term enrichment on genes with high regional specificity for each cluster (**Dataset S3**). Cluster Unknown 1 was enriched with genes related to ER stress, Unknown 2 had markers of Immune reactive cells, and Unknown 3 had non-retinal neuronal characteristics (**Fig. S2M-O**, **Dataset S3**). The Unknown 4 cells had 77 genes with high specificity to the cluster, but only two enriched gene sets "regulation of ion transmembrane transport" and "action potential" (**Dataset S3**). With such a small number of enriched gene sets, we were unable to make further conclusions about the identity of that cell cluster and have left them annotated as Unknown.

We next set out to understand how each treatment altered the distribution of cells across these novel clusters. We generated a heatmap in which treatments with similar cell type compositions were clustered together (**Fig. S2P**). In doing this, we found that for a small number of treatments, the majority of cells come from either the ER stressed cluster of cells or the Unknown

cluster of cells (**Fig. S2Q-R**). Interestingly, the treatments that led to the Unknown cluster include two histone deacetylase (HDAC) inhibitors (CI 994, SAHA) (38, 39). It's possible that these cells are deregulated without having yet experienced a change in fate towards a more specific cell type. The treatments that lead to increased cell counts in the ER stressed cluster include two bromodomain (acetylated lysine binders) inhibitors (I-BET 151 dihydrochloride, CPI 203) (40, 41). While these observations don't directly help us identify better treatments for reprogramming MG, they do help us find compounds that affect the molecular state of MG cells exposed to Ascl1 overexpression (2).

Validating sci-Plex hits in an *in vivo* neuronal regeneration paradigm.
We next aimed to assess whether the positive hits that increased neurogenesis from the *in vitro* sci-Plex screen could be validated *in vivo*. Before testing compounds from the *in vitro* screen *in vivo*, we sought to validate that *in vivo* MG express the signaling pathways targeted by our small molecule compounds during neurogenic reprogramming. We analyzed scRNA-seq libraries made from our *in vivo* regeneration experiments where we used mice engineered to express Ascl1 specifically in the MG (**Fig. 3A**), then induced retinal injury with an intravitreal injection of NMDA, and a co-injection of TSA (**Fig 3B**). The mice were sacrificed and GFP expressing cells were sorted and subjected to 10x scRNA-seq either 5, 9, or 21 days after injury (the day 5 and 9 libraries were originally published in (42)). Dimensionality reduction was performed to generate a UMAP from which clusters were defined and cell types were annotated using Marker genes (**Fig. 3C-D, Fig S3A-H, Table S1**). A small number of rod and cone cells are present even in the earliest time point and most likely are contaminating cells from the FACs sorting. As expected, with increasing time after injury, we observe greater numbers of MG-derived bipolar cells. This is most evident in the time between 9 and 21 days. However, even between 5 and 9 days there is a small increase in bipolar cells. Additionally, when pseudotime analysis was performed, a shift in the MG cluster towards a more mature state became apparent even by 9 days (**Fig. 3E**). Lastly, using the pseudotime analysis across all time points, we looked at how the expression of key target genes for each of the drugs are expressed throughout the reprogramming process (**Fig. 3F**). In all cases, at least some of the target genes are expressed early and decrease over time, making them ideal candidates for small molecule intervention.

Using the same mice as above, we aimed to validate five hits *in vivo* (the γ-secretase inhibitor DBZ, Lck and Src inhibitor WH-4-023, LKB1/AMPK activator metformin, the BMP inhibitor DMH-1, and the TGF-BR1 inhibitor SB43152) for their ability to increase neurogenic reprogramming of MG *in vivo*. We originally also identified RepSox as a hit, but because RepSox and SB43152 have the same target, we decided to only pursue SB43152. Ascl1 was induced in the MG with tamoxifen, retinal injury was performed by NMDA, and TSA was given in conjunction with one of the small molecule hits from the screen; animals were sacrificed two weeks later, and their retinas were assayed for lineage traced MG-derived cells (GFP+) and the retinal neuronal maker (Otx2+) (**Fig 3G**). Out of the compounds tested, two significantly boosted the number of Otx2+ neuronal cells (**Fig 3H-J**).

The first identified compound was DBZ, a γ-secretase/Notch inhibitor (**Fig. 3I**). This is consistent with reports in the chick retina where the γ-secretase inhibitor DAPT increased neuronal differentiation from proliferating MG (43–45). Inhibition of Notch is also well known to promote neural differentiation from retinal progenitors in mouse and human (46, 47). While this result was not unexpected, DBZ represents a new compound found to promote neurogenesis in the mammalian retina. The second positive hit, metformin, showed the biggest effect on MG-neurogenesis (**Fig. 3H-I**). In some retinas, metformin increased the rate of neurogenesis to 75% of the Ascl1-expressing MG, a higher rate than any of our previous pharmaceutical treatments. The MG derived neurons expressed Otx2, and were primarily located in the INL; this is similar to what we observe in the ANT treatment condition, and so it does not appear that metformin altered the fates of the MG-derived neurons; In addition, the neurons in the metformin treated retinas do not express markers of ganglion/amacrine cells (**Figure S3K**). These *in vivo* experiments thus confirm

that the *in vitro* sci-Plex screening is an effective method to identify new compounds that increase the regeneration potential of mammalian MG.

Discussion

Screening large numbers of chemical compounds has become a routine path to drug discovery, but limitations remain. Most high-throughput screening assays use relatively limited read-outs, such as cell morphology, proliferation or changes in expression of a reporter. Many assays cannot access molecular information about responding cells or identify factors that make a cell type resistant to a treatment. Single-cell transcriptomic assays overcome these hurdles, but the conventional protocols are costly and highly limited in sample number. Here, we demonstrate for the first time the utility of sci-Plex, an ultra-scalable scRNA-seq protocol, for studying reprogramming primary cells through screening drugs in low-input cultures and subsequently validating them *in vivo*. Our experiments both identified drugs that support reprogramming and revealed underlying biology important for the progression of glial cell reprogramming.

We first used sci-Plex to pinpoint the moment during *in vitro* reprogramming at which cells become committed towards a neurogenic cell fate independent of continued Ascl1 expression. Next, we tested 92 compounds across 3 doses each and identified 6 molecules of interest, two of which also had significant proneural effects *in vivo*. With our observation that cells no longer require Ascl1 to maintain their neuronal identity after a certain point along their reprogramming trajectory, we looked at the transcriptional regulators that were changing in their expression around this point and identified Myt1 as a potentially critical factor for commitment towards the neuronal fate. Myt1 is a zinc finger-containing DNA-binding transcription factor that is found specifically in neuronal cells and is important in neuronal differentiation (20, 48, 49). In neural stem cells, the Myt1 promoter is bound by Ascl1 and protein expression is induced following the overexpression of Ascl1 (20). Myt1 and its family member Myt1l function by binding to and repressing their target genes which include non-neuronal genes, progenitor genes, and regulators of Notch signaling (20, 50). Myt1l has also been associated with aiding in the *in vitro* reprogramming of fibroblasts to neurons (20, 50, 51). However, little is known about its role in the retina, and no previous reports indicate a direct role for Myt1 in committing cells to the neuronal fate after the removal of other proneural transcription factors. Additional work will be needed to determine whether Myt1 is the regulator holding cells in the neuronal fate after removal of Ascl1 in our Pulse experiment, but the depth of information that can be obtained by single cell sequencing provided us with an intriguing candidate gene.

The first hit of our screen was the Notch inhibitor DBZ. It targets the ability of gamma-secretase to cleave the intracellular domain of activated Notch receptors. While DBZ has not previously been used in retinal reprogramming studies, Notch is well-known to affect neurogenesis and neural regeneration in the retina. Pharmacological manipulation of Notch signaling has been used to alter the proliferative and neurogenic capacity of MG in fish and chick retina (43, 44, 52, 53). It is also interesting that Myt1, identified in our Pulse experiment as a factor that may prevent neuronal cells from returning to the progenitor fate, inhibits Notch signaling (20). That our screen recovered a gamma-secretase inhibitor, in line with the known role of Notch in the retina, confirmed the ability of our workflow to identify important regulators.

Unexpectedly, the second compound that increased neurogenesis *in vivo* was metformin. Mechanistically, metformin is typically thought to work via AMPK, and while used clinically for Type2 diabetes, many studies have noted its neuroprotective and anti-neuroinflammatory effects (54). In our screen, metformin increased the total number of cells recovered by sci-Plex, including those in the neurogenic precursor stage. Even with the increased number of cells recovered compared to other treatments, the small number of cells recovered from each treatment by sci-Plex made it difficult to identify confident DEGs. However, by leveraging followup experiments *in vivo* we did find that metformin had a clear effect on neurogenesis from Ascl1-reprogrammed MG. The effect we find on neurogenesis is consistent with the promotion of neurogenesis reported in another *in vitro* study using mouse cortical and hippocampal progenitors and human ESC-derived neural progenitors (55), and may in part be mediated by Gadd45g, via DNA methylation (56).

7

Moreover, metformin restored blood flow and vascular density in aged mice and promoted neurogenesis from the SVZ *in vivo and in vitro (57)*. Further investigations of this molecule in astrocyte to neuronal reprogramming in other regions of the CNS will be necessary to validate the utility of metformin in *in vivo* neural regeneration more generally.

Repairing the nervous system has been an elusive goal, and while progress is being made with transplantation of pluripotent stem cell derived neurons, there are many complexities in neural transplantation. Reprogramming glia to serve as a source of neural repair is a strategy utilized by non-mammalian vertebrates, and inspired by nature, we and others have shown that harnessing this latent neural regenerative capacity by proneural TF over-expression can revive the neuronal reprogramming program in mammals. Layering in the use of small molecules can increase the efficiency of such reprogramming, and we show here that screening through larger libraries of compounds at single-cell resolution *in vitro* can point us towards new *in vivo* hits. We are particularly excited by the future therapeutic potential of our compounds: metformin and DBZ; as well as the use of similar screening strategies for the identification of treatments in glial-based regeneration and wider contexts.

Materials and Methods

Mouse injections and husbandry
Mice were housed and treated under University of Washington Institutional Animal Care and Use Committee approved (UW-IACUC). Animals were maintained in groups of 2-5 per cage. For the *in vivo* experiments, *Glast-CreER:LNL-tTA;TetO-mAscl1-ires-GFP* mice are from mixed backgrounds of C57BL/6 and B6SJF1. The tetO-mAscl1-ires-GFP mice were a gift from M. Nakafuku (U. Cincinnati). Both sexes were used in all experiments and the mice used for injections were between the ages of P40-P60. To induce Ascl1 in MG *in vivo,* tamoxifen (Cayman Chemical, #13258-1G) was given intraperitoneally at 1.5mg per 100µl for four consecutive days. Intravitreal injections were performed on isoflurane anesthetized mice using a 32-gauge Hamilton syringe. All intravitreal injections were done at 2µl, and contained either NMDA (Sigma, #M3262-100MG) + drug or TSA (Tocris #1406/1) +drug. NMDA injections were done in 1µl volume at a concentration of 100mM. TSA injections were given in 1µl volume at a concentration of 1µg/µl. Drugs used were all from the Tocriscreen Stem Cell Library (Tocris, 7340) and were administered in 1µl of DMSO at 10mM. The mice were either randomized by animal tag number for injections (L1-4) or the vehicle (DMSO) was given to the left eye and the drug was given to the right eye (M). Blinding was performed for experiments.

Experiment	Treatment	Plot	N
M2	PBS (left eye)	DBZ	3
M2	DBZ (right eye)	DBZ	3
149	DBZ	DBZ	2
149	DMSO	DBZ	2
155	Metformin	Metformin	3
155	DMSO	Metformin	2
152	Metformin	Metformin	3
89	DMSO	Metformin	3
M1	PBS (left eye)	Non-sig	3
M1	SB431542 (right eye)	Non-sig	3
188	SB431542	Non-sig	2
188	DMH-1	Non-sig	3
168	WH-4-023	Non-sig	2

Primary cell culture, MG freezing, thawing, and plating
Muller glia cultures were derived from the retinas of Postnatal Day 11 (P11) rtTa:tetO-Ascl1-ires-GFP mice of both sexes. After retina harvest, the retinas were incubated for 7 min at 37°C in a solution of papain and deoxyribonuclease (DNase) (Worthington, #LK003172). Incubation was followed by trituration of the mixture to dissociate the cells, then to stop the reaction, an equal volume of ovomucoid (Worthington, #LK003182) was added. To isolate the cells, the solution was spun at 4°C at 300g for 10 minutes. Pelleted cells were resuspended in growth medium consisting of Neurobasal medium (Gibco, #10888-022), 10% tet-approved fetal bovine serum (tet-FBS) (Takara/Clontech, #631367), N2 (Gibco, #17502-048), 1 mM l-glutamine (Gibco, #25030-081), 1% penicillin-streptomycin (Gibco, #15140-122), and mouse epidermal growth factor (100 ng/ml) (R&D Systems, #2028-EG-200). Cells were plated in a six-well dish at a density of about 2 retinas per 10cm2 well, then incubated at 37°C. The entire volume of medium was changed every 48 hours until confluent or after 7 days. At confluence or after 7 days, cells were removed from the plate using TrypLE (Gibco, #12605-028), spun at 4°C at 300g for 10 minutes, then resuspended in a small volume of growth medium. The entire volume of cell suspension was added to a freezing medium containing 40% tet-FBS, and 10% dimethyl sulfoxide (DMSO), with the remaining 50% being the growth medium from the resuspension. The cells were then frozen for at least 24 hours at -80C before being moved to storage in liquid nitrogen for at least one day. Cells were thawed at room temperature, then spun at 300 RCF for 10 minutes. After thawing, cells were seeded in 500 uL of 10% tet-FBS growth medium in 24 well plates or in 250ul of the same medium in 48 well plates. Cells were grown for 24-48 hours in the growth medium until they appeared healthy.

Drug Treatment

Ascl1 Timecourse and Pulse
Once cells were confluent, the culture medium for all conditions was replaced with 1% tet-FBS-reduced growth medium. To activate the tetO-mediated transgenes, doxycycline (Sigma, #D9891-5G)
was added to the media at a concentration of 2 μg/mL at various time points over the course of 5 or 7 days.

Timecourse
Cells received doses of tet-FBS-reduced growth medium with doxycycline after 1, 2, 3, 4 or 5 days in culture. Once a treatment condition received its first dose of doxycycline, it continued to receive doses every 2 days for the remainder of the experiment. Prior to a condition's first dose of doxycycline, the cells were maintained in the reduced growth medium, which was replaced every 2 days. The control condition received no doxycycline and cultures were maintained in reduced growth medium replaced every 2 days.

Pulse
Cells received tet-FBS-reduced growth medium with doxycycline for 1, 2, 3, 4, or 5 days. Doxycycline was added to all conditions at the same time, Day 0, and all conditions remained in culture for 5 days. The media containing doxycycline was removed at each time point over the 5 day course and replaced with 1% tet-FBS-reduced medium for the remainder of the experiment.

Drug Treated Cells
Drugs were reconstituted in dimethyl sulfoxide (DMSO) with a starting concentration of 10 mM and were diluted to 2.5 mM, 250 uM, and 25 uM with a mixture of 50% DMSO and 50% PBS. Each well (48 well plate) of cells received a total volume of 250 uL of tet-FBS-reduced media with 1 uL of the designated treatment drug at each concentration (final concentration of drug 10 uM, 1

uM, 0.1 uM). Control wells received 250 uL of tet-FBS-reduced growth medium with the appropriate, equivalent DMSO concentration. Cells were collected after 5 days with an accutase dissociation. *(Further described in the cell collection section)*

Hashing for sci-Plex

To harvest cells for sci-Plex nuclei processing, the cells were rinsed either in 24- or 48-well plates with 200ul HBSS (Gibco, #14025-134), and then 200ul of Accutase (Sigma, #A6964-100ML). For experiments performed in 24-well plates, the accutase was incubated on the cells an additional 1 minute at room temperature before being removed. The cells were incubated with any residual accutase at 37°C for 5 minutes. Cells were then resuspended in 200 uL of 1% tet-FBS-reduced growth medium with a wide-bore P200 pipette tip to isolate single cells. The entire volume of the single cell suspension was transferred to a v-bottom 96-well plate on ice. The hashing of glia used a protocol adapted from the original sci-Plex publication(13). Briefly, dissociated cells were centrifuged at 600 x g for 5 minutes in 96-well v-bottom plates. Note that all centrifugation steps, including this one, were performed in a chilled swinging bucket centrifuge (4°C). Media was aspirated, and 200 uL 1 x dPBS (no calcium, no magnesium) was added to each well. The plate was centrifuged at 600x g for 5 minutes and the dPBS was pipetted off. To each well containing cells, 50 uL of CLB+hash solution (45 uL of Cold Lysis Buffer – 10mM Tris/HCl pH 7.4, 10mM NaCl, 3mM MgCl2 , 0.1% IGEPAL, 1% (v/v, Sigma-Aldrich, I8896), SuperaseIn RNase Inhibitor (20 U/µL, Ambion, AM2694), 1% (v/v) BSA (20 mg/ml, NEB, B9000S) + 5µL of hash oligo (10 uM, IDT)) was added and then mixed by pipetting up and down for 5-10 strokes. The plate was incubated on ice for 3 minutes, after which, 200 uL of fixation buffer (5% paraformaldehyde (EMS, cat. no. 50-980-493), 1.25x dPBS) was mixed with the nuclei by pipetting up and down for 10 strokes. The cells were incubated with the fixative for 15 minutes on ice during which the hashes were affixed to the nuclei. All nuclei from all wells were then collected into a single 15 or 50 mL conical tube, depending on the size of the experiment, and centrifuged for 5 minutes at 800xg. Pellets were resuspended in 1mL of NSB (Nuclei Buffer + SuperaseIn + BSA – 10mM Tris/HCl pH 7.4, 10mM NaCl, 3mM MgCl2 , 1% (v/v) BSA, 1% (v/v) SuperaseIn RNase Inhibitor), and centrifuged again for 5 minutes at 800 x g. One final wash with 1 mL of cold NSB was performed. Upon resuspension, nuclei were transferred to a 1.5 mL LoBind microcentrifuge tube (Eppendorf, Z666491) and counted using a hemocytometer. The 1.5 mL tube was placed within a 15 mL conical and centrifuged in a swinging bucket centrifuge for 5 minutes at 800 x g. The nuclei were resuspended in 500 uL of NSB and flash frozen in liquid nitrogen before being stored at -80C.

Sectioning and Immunostaining

For immunohistochemistry, whole eye globes were fixed for 30 minutes in 4% PFA after lens removal. Eyes were then soaked in 30% sucrose overnight and processed for sectioning the following day. For sectioning, retinas were frozen in O.C.T and cryosectioned at 18µm thickness. Slides were washed in PBS two times for 10 minutes and then primary antibodies were applied overnight in 10% normal horse serum (Vector Labs, #S-2000-20), 0.5% Triton-X-10 (Sigma, #T8787-100ML) and PBS. The following day sections were rinsed two times for 10 minutes in PBS and secondary antibodies were applied at a concentration of 1:1000 in PBS for 1 hour. Slides were washed again in PBS and then coverslipped using Fluromount-G (Southern Biotechnology, #0100-01)

Antibody/Stain	Source	Catalog #	RRID	Dilution
Primary				
Chicken anti-GFP	Abcam	Cat#: Ab13970	RRID: AB_300798	1:1000
Goat anti-OTX2	R&D Systems	Cat#: BAF1979	RRID: AB_2157171	1:500

Mouse anti-HuC/D	Invitrogen	Cat#: A-21271	RRID: AB_221448	1:500
Secondary				
Donkey anti-chicken 488	Jackson Immuno	Cat#: 703-545-155	RRID:AB_2340375	1:1000
Donkey anti-mouse 568	Life Technologies	Cat#: A10037	RRID:AB_2534013	1:1000
Donkey anti-goat 568	Life Technologies	Cat#: A11057	RRID:AB_2534104	1:1000
Stain				
DAPI	Sigma	Cat#: D9542	NA	1:7700

Microscopy and Cell counts
A Zeiss LSM880 confocal microscope was used to take images from the *in vivo* experiments. For quantifications, four images per retina at 20x objective were taken and both eyes were combined for a biological n. Statistical significance between treatments was determined using an unpaired t-test.

10x library preparation
Dissociated and GFP+ FACs sorted cells prepared 21 days after NMDA injury were subjected to the standard 10x workflow for Single Cell 3' v3.1 Dual Index Gene Expression kit (Dual Index Kit TT Set A 96 rxns, 10x Genomics, 1000215).

sci-RNA-seq
After hashing, the nuclei were subjected to the original 2-level sci-RNA-seq protocol(14) with minor modifications. Briefly, the hashed nuclei were thawed on ice, subjected to centrifugation at 800 x g for 5 minutes, the liquid was aspirated away, and then the nuclei were incubated on ice for 3 minutes in 500 uL of NSB + 0.2% Triton X-100 (ThermoFisher, A16046.AP). Permeabilized nuclei were centrifuged for 5 minutes at 800 x g, resuspended in 400 uL NSB, and counted using a hemocytometer. The desired number of nuclei were subjected to one final centrifugation step at 800 x g for 5 minutes. They were then resuspended to a concentration of ~800-3000 nuclei per uL across 3-4 x twin.tec™ 96 Well LoBind PCR Plates (Eppendorf, 0030129512) in NSB. The RT reaction was carried out using an increasing temperature gradient (4°C 2 min, 10°C 2 min, 20°C 2 min, 30°C 2 min, 40°C 2 min, 50°C 2 min, 55°C 15 min), but was otherwise the same as in Cao et. al.

All nuclei were pooled. DAPI (4′,6-diamidino-2-phenylindole, 3 uM final**)** (Invitrogen, D1306) was used to stain the DNA content of cells so that doublets and debris could be removed by sorting on the DAPI height vs DAPI area, and FSC vs SSC respectively using a FACSAria III cell sorter (BD Biosciences). Into each well of a twin.tec™ 96 Well LoBind PCR Plate, ~180 nuclei were sorted. This was performed across 4-5 plates depending on the experiment. Each of the wells that the nuclei were sorted into contained 5 uL of EB buffer (Qiagen, 19086), 0.5 uL of 5 x mRNA Second Strand Synthesis buffer (New England Biolabs, E6111L), and 0.25 uL of mRNA Second Strand Synthesis enzyme (New England Biolabs, E6111L). The plates were incubated at 16°C for 3 hours. Tagmentation was performed at 55°C for 5 minutes in 5.75 uL of Tagmentation mix (1.1 uL N7 loaded custom TDE1 enzyme (MacroLab, UC Berkeley) per 632.5 uL 2xTD buffer (20 mM Tris-HCl pH 7.6, 10 mM MgCl$_2$, 20% v/v Dimethyl Formamide (Sigma-Aldrich, 227056-100ML)).

11

The reaction was stopped with 12 uL of DNA binding buffer (Zymo Research, D4004-1-L). Ampure-based bead purification, PCR, and final library purification were performed as published previously (14). The library was visualized using a D1000 Screen Tape (Agilent Technologies, 5067-5583) and quantified by Qubit using Broad Range DNA reagents (Invitrogen, Q32853).

In-depth protocols can be found on protocols.io under the title.
Single cell RNA sequencing library preparation (2-level sci-RNA-seq)

Sequencing analysis

sci-Plex initial processing
The sci-Plex libraries were sequenced on an Illumina Nextseq550 (High Output 75 cycle kit) with 18 cycles for Read1, 10 cycles for each index, and 52 cycles for Read2. The reads were demultiplexed and then aggregated into individual cells using a pipeline developed by the Brotman Baty Institute (BBI) which is available at the bbi-lab github page under the bbi-dmux and bbi-sci repositories (https://github.com/bbi-lab). Custom code was used to incorporate the hash information outputted by the pipeline into a Monocle3 object.

Filtering and dimensionality reduction (Pulse vs Timecourse)
Cells with < 500 UMIs and > 20,000 UMIs were discarded. The ratio of the most common hash barcode to the second most common hash barcode was calculated (top_to_second_best_ratio). For the time course experiment, all cells with a top_to_second_best_ratio > 4 were retained. A cutoff of a top_to_second_best_ratio > 5 was used for the pulse experiment. Using Monocle3, the two datasets were combined with `combine_cds()` and subjected to dimensionality reduction to generate a 2D UMAP from 20 PCA dimensions, a UMAP mindist of 0.1, and 50 nearest neighbors. To best align the two datasets, `align_cds(alignment_group = "experiment", residual_model_formula_str = "~log10(n.umi)", preprocess_method = "PCA")` was applied after `preprocess_cds()` but before `reduce_dimension()` in the standard Monocle3 pipeline. Clustering was performed with a resolution of 6×10^{-4}, and cell types were assigned using marker genes (**Table S1**).

Pseudotime analysis (Pulse vs Timecourse)
Pseudotime scores were calculated with the root node set to the node at the center of the MG cluster. DEG analysis (`fit_models()`) was performed across pseudotime for cells with a pseudotime score of > 10 and < 20. Genes with an effect size of magnitude < 0.08 were filtered out. The remaining 250 genes with the lowest q-value were used in downstream analyses (**Dataset S1**). Expression heatmaps were constructed with ComplexHeatmap (58, 59) using all cells with a non-infinite pseudotime score. Cells were ordered by their pseudotime score and z-scores of the `normalized_counts()` are displayed.

Filtering and dimensionality reduction (Small Molecule Screen)
For both Collection 1 and 2, cells with < 500 UMIs, > 20,000 UMIs, or a top_to_second_best_ratio < 5 were discarded. Additionally, any cells with > 15% mitochondrial reads were removed from downstream analyses. The data from Collections 1 and 2 were combined as above and then subjected to dimensionality reduction with 30 PCA dimensions, a mindist of 0.1, and 100 nearest neighbors. Clustering was performed with `cluster_cells()` using a resolution of 1×10^{-4}. Marker genes were used to annotate cell types (**Table S1**).

Sub clustering of reprogramming MG cells (Small Molecule Screen)
The cells annotated as Bipolar and Reprogramming_MG were selected and dimensionality reduction was performed of the subset of cells with 30 PCA dimensions, a mindist of 0.1, and 12 nearest neighbors. A resolution of 5×10^{-4} was used for clustering. Common markers were used to assign cell types on a cluster by cluster basis (Table S1), but some clusters could not be assigned in this manner. To find the sets of genes that most specifically define these unknown

clusters, for each gene, the fraction of cells within a cluster that express the gene as well as the mean expression of that gene within a cluster were calculated. The mean expression values were then normalized to sum to one across all cell types for a given gene. This was used as input for Jensen Shannon distance calculations comparing the observed normalized expression distribution across cell types to simulated distributions in which all expression of a given gene comes from a single cell type. This was done for each cell type across all genes. Specificity scores were calculated by subtracting the Jensen Shannon distance from 1. The genes with a fraction expressing > 0.05 and a specificity of > 0.3 were categorized as highly specific for that cell type. For each Unknown cluster, the highly specific genes were used as input to `enrichGO()` from the clusterProfiler package with a pvalueCutoff of 0.01, qvalueCutoff = 0.05, and Benjamini Hoechberg adjustment using the org.Mm.eg.db OrgDb. The enriched biological processes ("BP") were then displayed by barplot.

Cell type quantification and fold change analysis
Heatmaps of cell type abundance across treatments were generated with `complexHeatmap()`. For fold-change calculations, the BP and NeuPre cell types were merged (Neuronal), as were the ProL (early) and ProL (late) cells (ProL). Any treatments with fewer than 20 cells recovered were discarded. A cell type by treatment matrix was generated and `size_factor()` adjusted. The matrix was used to calculate the fold-change in cell counts of each treatment compared to the Ascl1 only condition for all cell types. The total cell counts from each condition were also tabulated.

10x initial processing
The 10x libraries were sequenced on an Illumina Nextseq500 (150 cycle kit) with 28 cycles for Read1, 10 cycles for each index, and 90 cycles for Read2. The reads were processed using CellRanger (3.1.0)(60) with the default settings. The output was imported into Monocle3 (1.0.0)(18), and the D21 data was combined into a single object with the previously published D5 and D9 datasets(42).

Filtering and dimensionality reduction (*In vivo*)
Cells with < 2500 UMIs (D5 and D21) or < 3000 UMIs (D9) were discarded. Using Monocle3, the three datasets were combined with `combine_cds()` and subjected to dimensionality reduction to generate a 2D UMAP from 20 PCA dimensions, a UMAP mindist of 0.1, and 50 nearest neighbors. To best align the two datasets, `align_cds(alignment_group = "sample", residual_model_formula_str = "~log10(n.umi)", preprocess_method = "PCA")` was applied after `preprocess_cds()` but before `reduce_dimension()` in the standard Monocle3 pipeline. Clustering was performed with a resolution of 6×10^{-4}, and cell types were assigned using marker genes (**Table S1**).

Pseudotime analysis (*In vivo*)
Pseudotime scores were calculated with the root node set to the node at the center of the MG cluster. Expression heatmaps were constructed with ComplexHeatmap (58, 59) using all cells with a non-infinite pseudotime score. Cells were ordered by their pseudotime score and z-scores of the `normalized_counts()` are displayed.

Resource availability
Lead contact
Further information and requests for resources and reagents should be directed to and will be fulfilled by the lead contact, Thomas A. Reh (tomreh@uw.edu).
Materials availability
No unique materials were generated by this study.
Data availability
The single cell sequencing data have been deposited at GEO: GSE239731. All code used for the analysis has been uploaded to github at https://github.com/atresen/sci-plex_glia/tree/main.

References

1. L. Todd, T. A. Reh, Comparative Biology of Vertebrate Retinal Regeneration: Restoration of Vision through Cellular Reprogramming. *Cold Spring Harb. Perspect. Biol.* **14** (2022).

2. N. L. Jorstad, *et al.*, Stimulation of functional neuronal regeneration from Müller glia in adult mice. *Nature* **548**, 103–107 (2017).

3. C. Lentini, *et al.*, Reprogramming reactive glia into interneurons reduces chronic seizure activity in a mouse model of mesial temporal lobe epilepsy. *Cell Stem Cell* **28**, 2104–2121.e10 (2021).

4. J. Pollak, *et al.*, ASCL1 reprograms mouse Müller glia into neurogenic retinal progenitors. *Development* **140**, 2619–2631 (2013).

5. N. L. Jorstad, *et al.*, STAT Signaling Modifies Ascl1 Chromatin Binding and Limits Neural Regeneration from Muller Glia in Adult Mouse Retina. *Cell Rep.* **30**, 2195–2208.e5 (2020).

6. L. Todd, *et al.*, Efficient stimulation of retinal regeneration from Müller glia in adult mice using combinations of proneural bHLH transcription factors. *Cell Rep.* **37**, 109857 (2021).

7. L. Todd, *et al.*, Reprogramming Müller glia to regenerate ganglion-like cells in adult mouse retina with developmental transcription factors. *Sci Adv* **8**, eabq7219 (2022).

8. Y. Ueki, *et al.*, Transgenic expression of the proneural transcription factor Ascl1 in Müller glia stimulates retinal regeneration in young mice. *Proc. Natl. Acad. Sci. U. S. A.* **112**, 13717–13722 (2015).

9. S. Gascón, *et al.*, Identification and Successful Negotiation of a Metabolic Checkpoint in Direct Neuronal Reprogramming. *Cell Stem Cell* **18**, 396–409 (2016).

10. J. Janowska, *et al.*, Directed glial differentiation and transdifferentiation for neural tissue regeneration. *Exp. Neurol.* **319**, 112813 (2019).

11. L. Cheng, *et al.*, Direct conversion of astrocytes into neuronal cells by drug cocktail. *Cell Res.* **25**, 1269–1272 (2015).

12. L. Gao, *et al.*, Direct Generation of Human Neuronal Cells from Adult Astrocytes by Small Molecules. *Stem Cell Reports* **8**, 538–547 (2017).

14

13. S. R. Srivatsan, *et al.*, Massively multiplex chemical transcriptomics at single cell resolution. *Science* **6234**, 1–13 (2019).

14. J. Cao, *et al.*, Comprehensive single-cell transcriptional profiling of a multicellular organism. *Science* **357**, 661–667 (2017).

15. L. M. Saunders, *et al.*, Deep molecular, cellular and temporal phenotyping of developmental perturbations at whole organism scale https:/doi.org/10.1101/2022.08.04.502764.

16. M. W. Dorrity, *et al.*, Proteostasis governs differential temperature sensitivity across embryonic cell types. *bioRxiv*, 2022.08.04.502669 (2022).

17. A. Tresenrider, *et al.*, Single-cell sequencing of individual retinal organoids reveals determinants of cell fate heterogeneity. *bioRxiv*, 2023.05.31.543087 (2023).

18. J. Cao, *et al.*, The single-cell transcriptional landscape of mammalian organogenesis. *Nature* **566**, 496–502 (2019).

19. C. Roschger, C. Cabrele, The Id-protein family in developmental and cancer-associated pathways. *Cell Commun. Signal.* **15**, 7 (2017).

20. F. F. Vasconcelos, *et al.*, MyT1 Counteracts the Neural Progenitor Program to Promote Vertebrate Neurogenesis. *Cell Rep.* **17**, 469–483 (2016).

21. J. Lee, *et al.*, A Myt1 family transcription factor defines neuronal fate by repressing non-neuronal genes. *Elife* **8** (2019).

22. R. B. Hufnagel, T. T. Le, A. L. Riesenberg, N. L. Brown, Neurog2 controls the leading edge of neurogenesis in the mammalian retina. *Dev. Biol.* **340**, 490–503 (2010).

23. H. Liu, M. Aramaki, Y. Fu, D. Forrest, "Chapter Eight - Retinoid-Related Orphan Receptor β and Transcriptional Control of Neuronal Differentiation" in *Current Topics in Developmental Biology*, D. Forrest, S. Tsai, Eds. (Academic Press, 2017), pp. 227–255.

24. A. Usui, *et al.*, Expression of Sox4 and Sox11 is regulated by multiple mechanisms during retinal development. *FEBS Lett.* **587**, 358–363 (2013).

25. Y. Jiang, *et al.*, Transcription factors SOX4 and SOX11 function redundantly to regulate the development of mouse retinal ganglion cells. *J. Biol. Chem.* **288**, 18429–18438 (2013).

26. H. Liu, *et al.*, An isoform of retinoid-related orphan receptor β directs differentiation of retinal amacrine and horizontal interneurons. *Nat. Commun.* **4**, 1813 (2013).

27. A. Swaroop, D. Kim, D. Forrest, Transcriptional regulation of photoreceptor development and homeostasis in the mammalian retina. *Nat. Rev. Neurosci.* **11**, 563–576 (2010).

28. J. Milano, *et al.*, Modulation of notch processing by gamma-secretase inhibitors causes intestinal goblet cell metaplasia and induction of genes known to specify gut secretory lineage differentiation. *Toxicol. Sci.* **82**, 341–358 (2004).

29. J. Hao, *et al.*, In vivo structure-activity relationship study of dorsomorphin analogues identifies selective VEGF and BMP inhibitors. *ACS Chem. Biol.* **5**, 245–253 (2010).

15

30. J. K. Ichida, *et al.*, A small-molecule inhibitor of tgf-Beta signaling replaces sox2 in reprogramming by inducing nanog. *Cell Stem Cell* **5**, 491–503 (2009).

31. F. Gellibert, *et al.*, Identification of 1,5-naphthyridine derivatives as a novel series of potent and selective TGF-beta type I receptor inhibitors. *J. Med. Chem.* **47**, 4494–4506 (2004).

32. G. J. Inman, *et al.*, SB-431542 is a potent and specific inhibitor of transforming growth factor-beta superfamily type I activin receptor-like kinase (ALK) receptors ALK4, ALK5, and ALK7. *Mol. Pharmacol.* **62**, 65–74 (2002).

33. N. J. Laping, *et al.*, Inhibition of transforming growth factor (TGF)-beta1-induced extracellular matrix with a novel inhibitor of the TGF-beta type I receptor kinase activity: SB-431542. *Mol. Pharmacol.* **62**, 58–64 (2002).

34. T. W. Theunissen, *et al.*, Systematic identification of culture conditions for induction and maintenance of naive human pluripotency. *Cell Stem Cell* **15**, 471–487 (2014).

35. K. Clark, *et al.*, Phosphorylation of CRTC3 by the salt-inducible kinases controls the interconversion of classically activated and regulatory macrophages. *Proc. Natl. Acad. Sci. U. S. A.* **109**, 16986–16991 (2012).

36. M. W. Martin, *et al.*, Novel 2-aminopyrimidine carbamates as potent and orally active inhibitors of Lck: synthesis, SAR, and in vivo antiinflammatory activity. *J. Med. Chem.* **49**, 4981–4991 (2006).

37. A. F. G. Cicero, E. Tartagni, S. Ertek, Metformin and its clinical use: new insights for an old drug in clinical practice. *Arch. Med. Sci.* **8**, 907–917 (2012).

38. A. J. Kraker, *et al.*, Modulation of histone acetylation by [4-(acetylamino)-N-(2-amino-phenyl) benzamide] in HCT-8 colon carcinoma. *Mol. Cancer Ther.* **2**, 401–408 (2003).

39. L. M. Butler, *et al.*, Suberoylanilide hydroxamic acid, an inhibitor of histone deacetylase, suppresses the growth of prostate cancer cells in vitro and in vivo. *Cancer Res.* **60**, 5165–5170 (2000).

40. B. N. Devaiah, *et al.*, BRD4 is an atypical kinase that phosphorylates serine2 of the RNA polymerase II carboxy-terminal domain. *Proc. Natl. Acad. Sci. U. S. A.* **109**, 6927–6932 (2012).

41. M. A. Dawson, *et al.*, Inhibition of BET recruitment to chromatin as an effective treatment for MLL-fusion leukaemia. *Nature* **478**, 529–533 (2011).

42. L. Todd, C. Finkbeiner, C. K. Wong, M. J. Hooper, T. A. Reh, Microglia Suppress Ascl1-Induced Retinal Regeneration in Mice. *Cell Rep.* **33**, 108507 (2020).

43. S. Hayes, B. R. Nelson, B. Buckingham, T. A. Reh, Notch signaling regulates regeneration in the avian retina. *Dev. Biol.* **312**, 300–311 (2007).

44. K. Ghai, C. Zelinka, A. J. Fischer, Notch signaling influences neuroprotective and proliferative properties of mature Müller glia. *J. Neurosci.* **30**, 3101–3112 (2010).

45. L. Todd, N. Squires, L. Suarez, A. J. Fischer, Jak/Stat signaling regulates the proliferation and neurogenic potential of Müller glia-derived progenitor cells in the avian retina. *Sci. Rep.* **6**, 35703 (2016).

46. C. Finkbeiner, *et al.*, Single-cell ATAC-seq of fetal human retina and stem-cell-derived retinal organoids shows changing chromatin landscapes during cell fate acquisition. *Cell Rep.* **38**, 110294 (2022).

47. B. R. Nelson, B. H. Hartman, S. A. Georgi, M. S. Lan, T. A. Reh, Transient inactivation of Notch signaling synchronizes differentiation of neural progenitor cells. *Dev. Biol.* **304**, 479–498 (2007).

48. E. J. Bellefroid, *et al.*, X-MyT1, a Xenopus C2HC-type zinc finger protein with a regulatory function in neuronal differentiation. *Cell* **87**, 1191–1202 (1996).

49. J. G. Kim, L. D. Hudson, Novel member of the zinc finger superfamily: A C2-HC finger that recognizes a glia-specific gene. *Mol. Cell. Biol.* **12**, 5632–5639 (1992).

50. M. Mall, *et al.*, Myt1l safeguards neuronal identity by actively repressing many non-neuronal fates. *Nature* **544**, 245–249 (2017).

51. T. Vierbuchen, *et al.*, Direct conversion of fibroblasts to functional neurons by defined factors. *Nature* **463**, 1035–1041 (2010).

52. C. Conner, K. M. Ackerman, M. Lahne, J. S. Hobgood, D. R. Hyde, Repressing notch signaling and expressing TNFα are sufficient to mimic retinal regeneration by inducing Müller glial proliferation to generate committed progenitor cells. *J. Neurosci.* **34**, 14403–14419 (2014).

53. J. Wan, R. Ramachandran, D. Goldman, HB-EGF is necessary and sufficient for Müller glia dedifferentiation and retina regeneration. *Dev. Cell* **22**, 334–347 (2012).

54. M. Markowicz-Piasecka, *et al.*, Metformin - a Future Therapy for Neurodegenerative Diseases : Theme: Drug Discovery, Development and Delivery in Alzheimer's Disease Guest Editor: Davide Brambilla. *Pharm. Res.* **34**, 2614–2627 (2017).

55. J. Wang, *et al.*, Metformin activates an atypical PKC-CBP pathway to promote neurogenesis and enhance spatial memory formation. *Cell Stem Cell* **11**, 23–35 (2012).

56. L. Zhang, *et al.*, Gadd45g, A Novel Antidepressant Target, Mediates Metformin-Induced Neuronal Differentiation of Neural Stem Cells Via DNA Demethylation. *Stem Cells* **40**, 59–73 (2022).

57. X. Zhu, *et al.*, Metformin improves cognition of aged mice by promoting cerebral angiogenesis and neurogenesis. *Aging* **12**, 17845–17862 (2020).

58. Z. Gu, R. Eils, M. Schlesner, Complex heatmaps reveal patterns and correlations in multidimensional genomic data. *Bioinformatics* **32**, 2847–2849 (2016).

59. Z. Gu, Complex heatmap visualization. *Imeta* **1** (2022).

60. G. X. Y. Zheng, *et al.*, Massively parallel digital transcriptional profiling of single cells. *Nat. Commun.* **8**, 14049 (2017).
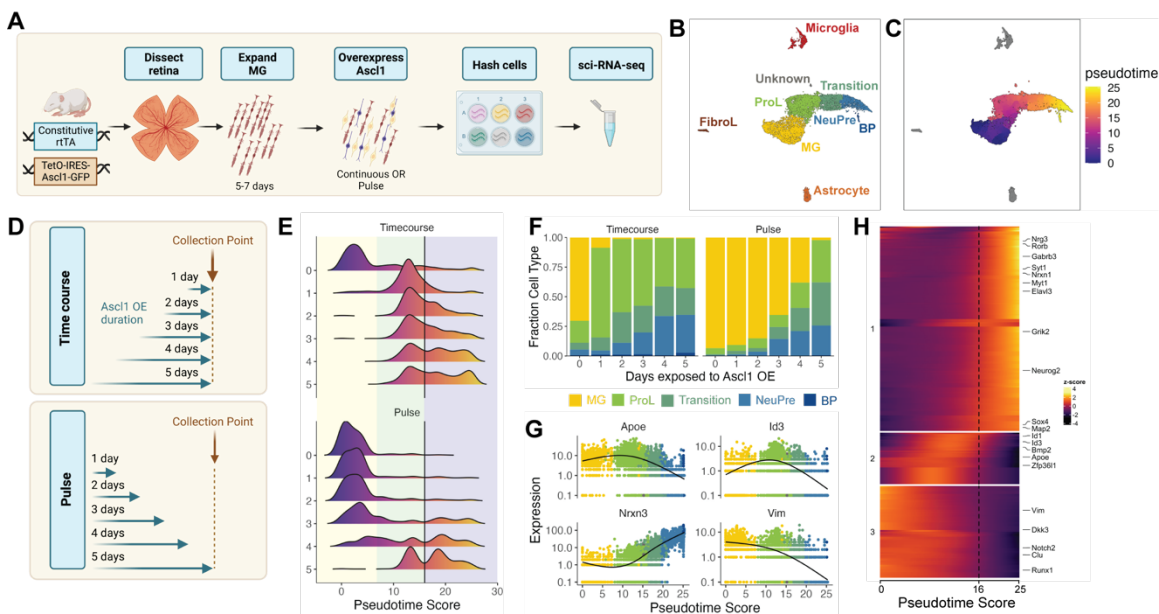
Figures and Tables

Figure 1. *sci-Plex captures the in vitro temporal dynamics of neurogenic reprogramming from MG.* **A)** Schematic of the sci-Plex experimental design for assaying reprogramming MG isolated from P11 mice. **B)** Combined UMAP of cells from the Timecourse and Pulse experiments. Cells are colored by cell type. **C)** UMAP displaying the pseudotime scores that were calculated for the MG to Bipolar trajectory. **D)** Schematic depicting the timing and duration of Ascl1 OE in the Timecourse and Pulse experiments. **E)** Histograms displaying the frequency of cells with each pseudotime score across Ascl1 OE conditions. The vertical black lines are at pseudotime score 16. The yellow region corresponds to the MG, the green region corresponds to the ProL cells, and the purple region reflects cells from the Transition to BP cell state. **F)** Stacked bar plot of the cell type composition across all Ascl1 OE conditions. The colors represent the cell types as indicated. Only the MG and MG-derived cell types are included. **G)** Gene expression plots along pseudotime for genes of interest. Each point represents an individual cell's expression of the indicated gene. The cells are colored by cell type as in F. **H)** Gene expression heatmap for the top 250 DEGs as assessed across a pseudotime score of 10-20. The dashed line is at pseudotime score 16. All cells with a non-infinite pseudotime score are ordered by pseudotime score along the x-axis. Genes were clustered by k-means into 3 clusters.
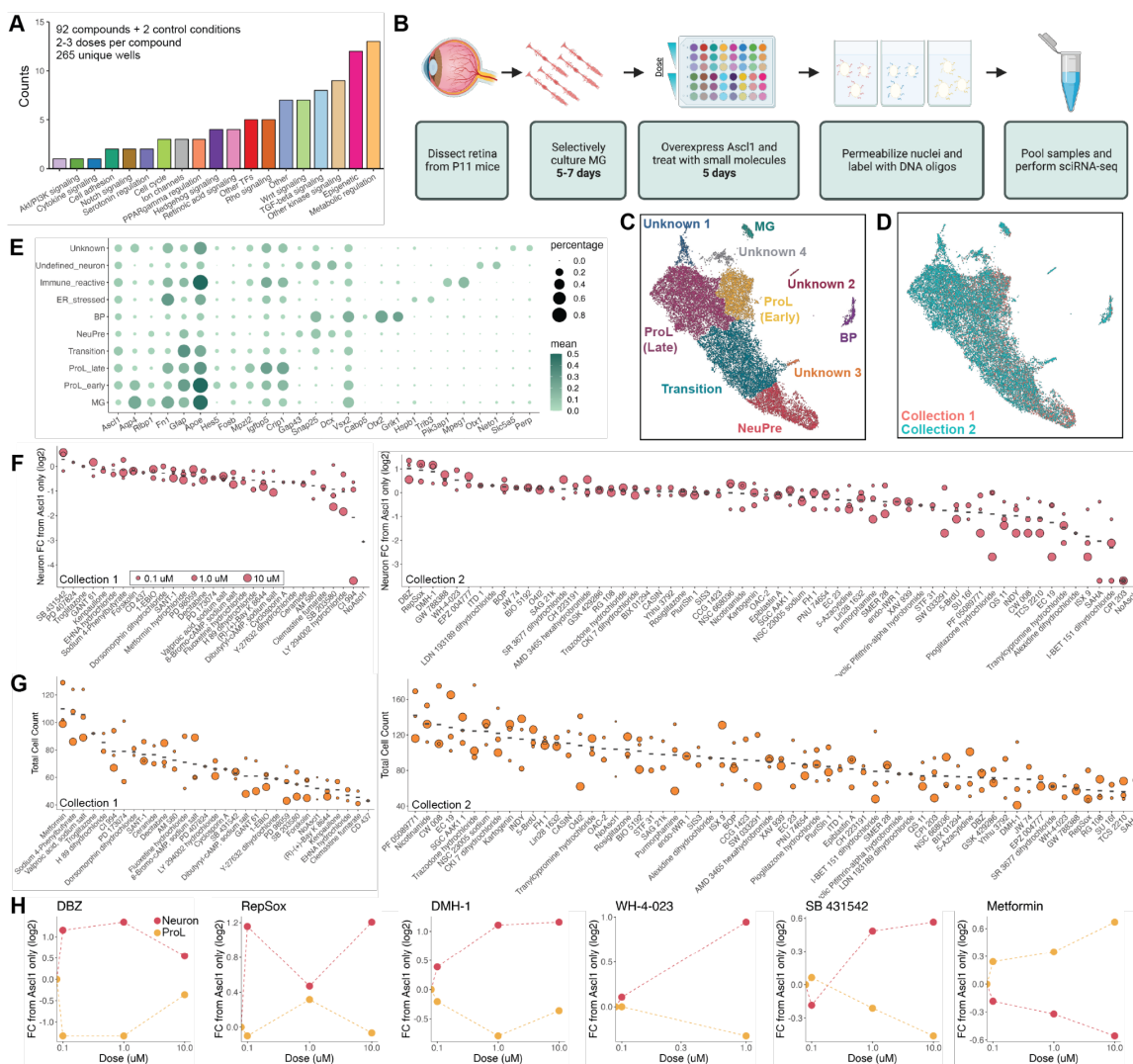
Figure 2. sci-Plex as a screen to identify small molecules that affect Ascl1-dependent MG reprogramming. A) Bar plot representing the distribution of targets for the 92 compounds included in the screen. **B)** Schematic of the experimental design for the small molecule screen. **C)** UMAP of the MG and MG-derived cell types. Cells are colored by cell type. **D)** UMAP from C with cells colored by collection. **E)** Dot plot of the genes used to define the MG-derived cell types from the screen. Dot size indicates the percent of cells that express the gene of interest. The color indicates the log10 mean UMIs per cell. **F)** Quantification of the fold change in Neuron cell counts between each indicated condition and the Ascl1 only control. The plots from Collection 1 and Collection 2 used only the control wells collected on their respective days. The dose of each compound is indicated by the size of the dot. **G)** Quantification of the total cell counts for each treatment. The compound's dose is indicated by the size of the dot. **H)** Plots displaying the fold change of Neuron (red) and ProL (orange) cell counts compared to Ascl1 only across all doses for the top hits from the screen. All conditions in which at least 20 cells were recovered are displayed.
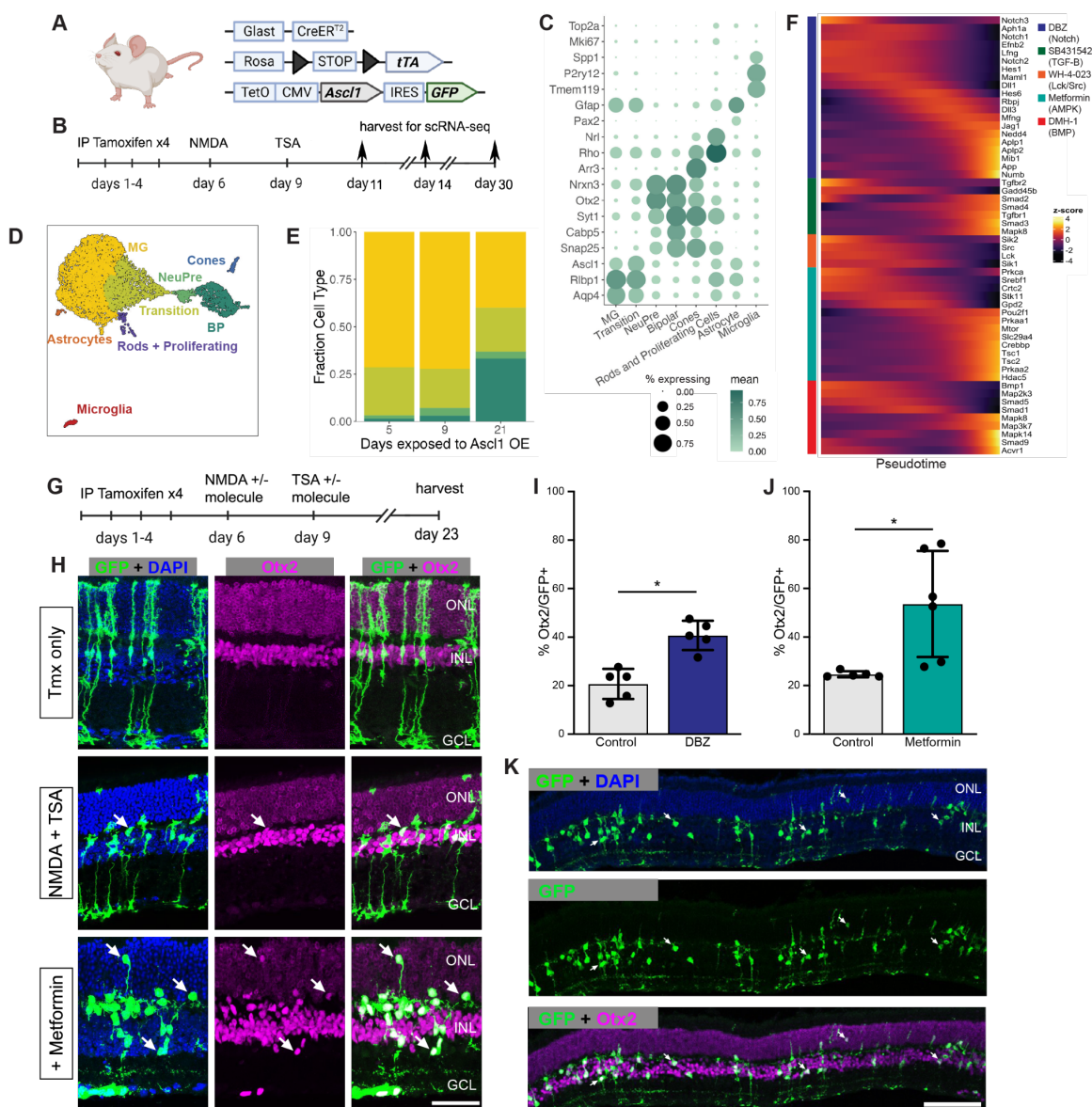
Figure 3. Validation of sci-plex hits in an *in vivo* neuronal regeneration paradigm. A) Schematic of the transgenic mouse used to induce Ascl1 and GFP specifically in MG. **B)** Experimental paradigm for testing the *in vivo* dynamics of Ascl1-dependent MG reprogramming. **C)** Dot plot of the genes used to define the major cell types found in the reprogramming cells *in vivo* across all timepoints. The size of the dot indicates the percent of cells that express the gene of interest. The color indicates the log10 mean UMIs per cell. **D)** An integrated UMAP of the cells recovered from *in vivo* reprogramming 5, 9, or 21 days after NMDA treatment. Cells are colored by cell type. E) Stacked bar plot of the cell type composition across *in vivo* Ascl1 OE durations. The colors represent the cell types as in D. Only the MG and MG-derived cell types are included. **F)** Heatmap of the *in vivo* expression of genes related to the pathways regulated by the top small molecules hits from the *in vitro* screen. Reprogramming cells are ordered along pseudotime. The row normalized z-score was calculated from size factor normalized gene expression counts. **G)** Experimental paradigm for testing the *in vivo* effect of hit compounds on reprogramming. **H)** Representative sections of retina after Ascl1 only, Ascl1/NMDA/TSA or

20

Ascl1/NMDA/TSA/Metformin treatment. Immunostaining for GFP (green) and Otx2 (purple) show MG-derived cells (GFP+) expressing the neuronal marker Otx2. Scale bar =50μm. **I)** Quantification of the percentage of GFP+ MG-derived cells that express the neuronal marker in Ascl1/NMDA/TSA (control) versus the addition of Metformin (p=0.017). Statistical significance was determined using an unpaired t-test. Height of the bar indicates the mean, and the error bars indicate the standard deviation. **J)** Quantification of the percentage of GFP+/Otx2+ cells in control versus DBZ treatment (p=0.0009). Statistical significance was determined using an unpaired t-test. Height of the bar indicates the mean, and the error bars indicate the standard deviation. **K)** Representative widefield image of GFP+ MG-derived neurons (GFP+/Otx2+) showing the widespread stimulation of neurogenesis in metformin treated retinas. Scale bar is 100μm.